JOURNAL DE PHYSIQUE IV
Colloque C4, supplément au Journal de Physique III, Vol. 1, novembre 1991

EFFECT OF THERMAL CYCLING ON THE MARTENSITIC TRANSFORMATION OF βCu-Zn-Al CONTAINING γ PRECIPITATES

J. PONS, F.C. LOVEY* and E. CESARI

Dept. de Fisica, Universitat de les Illes Balears, Ctra de Valldemossa, Km. 7.5 E-07071 Palma de Mallorca, Spain

**Division Metales, Centro Atomico Bariloche, 8400 S. C. de Bariloche, Argentina*

Abstract - We present a calorimetric and TEM study of the thermal cycling effects on the martensitic transformation in β Cu-Zn-Al single crystals containing different distributions of γ-phase precipitates. The calorimetric results show a high reproducibility of the transformation during cycling (up to 200 cycles) for dense distributions of coherent precipitates, and a shift towards higher temperatures (mainly the direct transformation) for a distribution of precipitates of bigger size. Arrays of dislocations similar to those formed in precipitate-free specimens were observed in this study, although in a small quantity. Moreover, complex dislocation networks in the matrix surrounding the precipitates were also observed. The effects of both kinds of dislocation arrays on the martensitic transformation are discussed.

1. Introduction

Successive thermal cycling through a thermoelastic martensitic transformation is known to produce an evolution of the transformation characteristics [1-3]. In Cu-Zn-Al shape memory alloys some changes in transformation temperatures and heat exchanged were reported [4]. From a microscopic point of view, the defects introduced during cycling were also analysed [5-7] and in a recent work the changes of the transformation temperatures were related to the dislocation arrays formed during cycling [7]. On the other hand, the presence of γ-phase precipitates inside the parent β phase also affects the transformation behaviour [8-10]. The thermal cycling of Cu-Zn-Al single crystals containing different distributions of γ-precipitates was studied from a macroscopic point of view by means of calorimetry [11]. The evolution of transformation characteristics was found to be different for the three distributions of precipitates studied, depending on the size, coherency and density of precipitates, and also different from that obtained in precipitate-free specimens [4].

In this work we present a first analysis, by TEM, of the defects formed during cycling in Cu-Zn-Al single crystals containing distributions of precipitates similar to those analysed in [11]. We compare the dislocation arrays with those observed in material free of precipitates [7]. The evolutions of transformation temperatures can be related to the dislocation arrays observed in each case.

2. Experimental procedure

Single crystals of composition 68.0% Cu - 15.7% Zn - 16.3% Al (at%, e/a=1.48, nominal Ms = 263 K) were grown by the Bridgman method. Three rods of 6 mm in diameter and 3 cm in length were cut with a low speed diamond saw. The specimens were submitted to the following thermal treatments:

- After 20' at 850 ºC, air cooling to 500 ºC and quench into ice-water at 0 ºC (TTB), followed by an air heating to 400 ºC for 20 s and subsequent quenching into water at room temperature. Applied to specimen 1.
- The same TTB treatment as in specimen 1 followed by a flash heating in a melted salt bath at 400 ºC for 20s and quenching into water at room temperature. Applied to sample 2.

- After 20' at 850 ºC, quench into water at room temperature (TTD), followed by a flash heating in a salt bath at 400 ºC for 70s and quench into water at room temperature. Applied to sample 3.

From these original rods, samples suitable for calorimetry were cut, having 2 mm in thickness. The remaining ingots were oriented by means of X-ray diffraction (Laue method). Several slices of 0.4mm in thickness were cut on the $(100)_\beta$ plane for observation by TEM. In this way, the formation of surface martensite and its effects on the image were avoided [12].

A calorimetric study analogous to that performed in [11] was repeated for specimens 2 and 3 in order to avoid uncertainties when comparing with the previous calorimetric results due to slight differences that could appear in the precipitate distributions. The calorimetric samples were mechanically and electrolitically polished before the calorimetric runs. Two transformation cycles were recorded at a rate of 0.3-0.4 K/min. Afterwards, these samples as well as the remaining rods were simultaneously cycled between 190 and 310K at a rate ~2 K/s up to 200 cycles. In this range, the complete direct and reverse transformation takes place for all specimens. At cycles 10, 50 100 and 200 the process was stopped in order to record at least two calorimetric cycles and cut several slices from the rods for TEM observation. In this way, the transformation cycling is performed in bulk specimens, avoiding possible effects of thin foil.

TEM samples were prepared by double-jet electropolishing at room temperature in a solution containing phosphoric acid, ethanol, propanol and urea at 8V and observed in a Hitachi H-600 100 kV electron microscope. The dislocations were observed in bright field two-beam condition under the [110] or $[\bar{1}10]$ operating reflections near the [001] zone axis and the <011>, <200> reflections close to the corresponding <011> zone axis. The Burgers vectors, **b**, were obtained by matching to computer simulated images taken from the paper of Sade et al. [15].

3. Results and discussion

3.1 Calorimetric results

The transformation temperatures, as well as the heats exchanged and entropy changes obtained at the different stages of cycling for samples 2 and 3 are shown in table 1.

Table 1. Transformation temperatures, heats exchanged (Q) and entropy changes (ΔS) obtained at the different stages of cycling. The Q and ΔS values are the average between those of the direct and inverse transformation and are given per sample unit mass. Uncertainties: ±1 K for temperatures, ±10 J/mol for Q and ±0.04 J/molK for ΔS

Cycle	Ms (K)	Mf (K)	As (K)	Af (K)	Q (J/mol)	ΔS (J/molK)
Sample 2. TTB/20s						
1	257	202	213	262	268	1.19
10	256	204	215	263	260	1.12
50	255	205	215	262	260	1.11
100	256	206	214	264	255	1.09
200	257	206	214	264	256	1.09
Sample 3. TTD/70s						
1	264	241	252	275	279	1.08
10	265	239	252	277	282	1.09
50	267	242	253	278	279	1.07
100	269	244	252	278	266	1.02
200	269	244	253	277	246	0.94

The results shown in table 1 present the same behaviour than those of [11]: high stability of the hysteresis loop during cycling of sample 2, as was also observed in sample 1, and a shift of the transformation temperatures (mainly the direct transformation ones) to higher temperatures for sample 3. The decrease in Q and ΔS can be related to the presence of retained martensite as it occurs in precipitate-free samples [4].

3.2 Microscopy observations

The as-treated sample 1 (with no transformation cycles) shows a distribution of small spheroidal precipitates (size ~150 Å) coherent with the matrix. The distribution of precipitates is quite homogeneous in most of the zones (fig. 1a), although some areas with a lesser number of precipitates of a bigger size, and other zones with complete absence of precipitates exist. In the precipitate-free areas, some dislocations have been observed. In sample 2, a distribution of precipitates of ~300Å mean size forms (fig. 1b). This larger size shows the better efficiency when performing the flash heating at 400 ºC in a salt bath than in air. In sample 3, the distribution of precipitates is more heterogeneous. Isolated precipitates or close groups of several of them (up to 5) can be observed (fig. 1c), separated by extended zones completely free of precipitates. In these areas, some dislocations can be seen before cycling, which are formed during the quenching from 1120K, as observed also in [7]. The flash heating to 670K does not eliminate these dislocations. The precipitates are cuboidal and have much bigger size (0.3-0.5 μm), losing the coherency with the matrix. The biggest precipitates show a four-leaves clover shape. This is the first stage for a precipitate division from a cube to an octet of smaller precipitates.

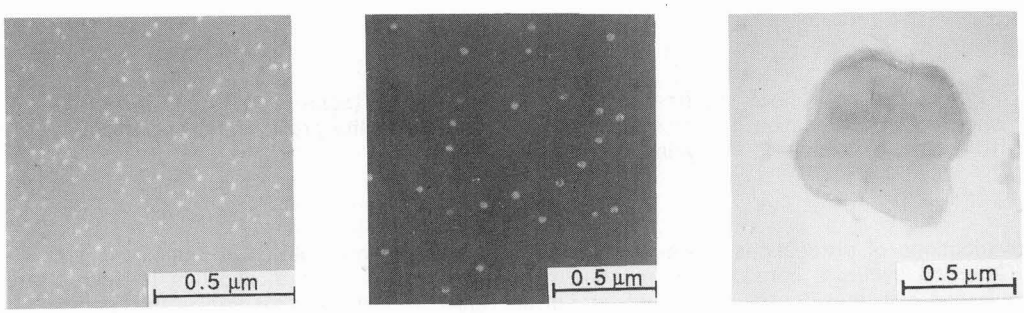

Figure 1. Distributions of precipitates obtained after the thermal treatments: a) sample 1, (dark field), b) sample 2 (dark filed), c) sample 3 (bright field). Zone axis [011]

Optical microscopy observations show that the martensite plates are thinner and shorter than in precipitate-free specimens, being this effect more pronounced as the precipitate size increases. Nevertheless, the plate size is large enough to absorb the precipitates in specimens 1 and 2, whereas in sample 3 the precipitates size is so big that the martensite plates can not overcome them completely. In this case, a structure of tiny plates are formed in between the precipitates.

During thermal cycling, dislocation arrays form in the matrix between the precipitates and more complex arrays of short dislocations are observed in the matrix surrounding the precipitates, connecting the precipitates with the foil surfaces (fig. 2). In the latter case, the dislocations are distributed in an isotropic way around the precipitates (no special directions with higher density of defects have been seen).

In all cases the dislocations have the $\mathbf{b}=\langle 100\rangle_\beta$ Burgers vector and the dislocation line lies, generally, on $\mathbf{u}=\langle 111\rangle_\beta$ direction. These dislocations are of the same kind observed in precipitate-free samples [5-7]. Some segments lying on $\mathbf{u}=\langle 100\rangle_\beta$ directions can also be observed, particularly in the precipitate vicinities. Most dislocations are composed of several segments with different directions, rarely a unique segment crosses completely from one foil surface to the other. This fact, which was not so often observed

in precipitate-free specimens [7], could be a consequence of the stress field created by the precipitates in the near matrix.

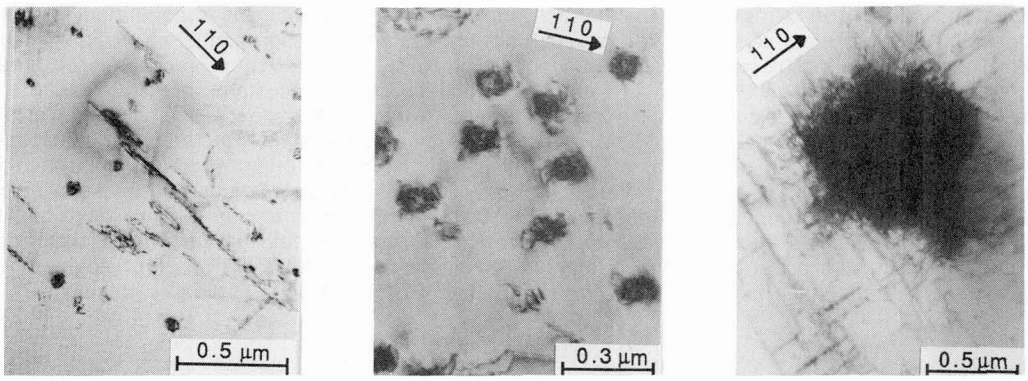

Figure 2. Bright field two-beam condition micrographs (zone axis [001], **g**=[110]) showing the dislocation networks in the matrix surrounding the precipitates. a) sample 1, 10 cycles; b) sample 2, 10 cycles, c) sample 3, 10 cycles.

The distributions of dislocations observed in the matrix between precipitates in samples 1 and 2 are alike. After 10 cycles a considerable number of dislocations are formed, showing in several areas accumulations of higher density than in the rest of the specimen, although, generally, the accumulations are less dense than those found in samples without precipitates [7]. Increasing the number of cycles, the number and size of such arrays also increase, as well as the mean density in the rest of specimen, showing a saturation between 100 and 200 cycles (mean density of 18 $\mu m/\mu m^3$, being 26 $\mu m/\mu m^3$ for precipitate-free samples, obtained in the way explained in [7]). Nevertheless, after 100 or 200 cycles areas having a very low density of dislocations can still be seen (fig. 3). In sample 3, large zones free of precipitates exist. In this zones dislocations are also formed during cycling, distributed in much smaller and less dense arrays than in precipitate-free samples [7] (fig. 4). Generally, the dislocation density is higher near the precipitates, and very low (even after 200 cycles) far from them.

3.3 Relation between martensite plates, precipitates and dislocation arrays

Due to the intrinsic deformation associated to the transformation, stresses are created between the precipitates and the surrounding martensite [13], which are too high to be completely accommodated in an elastic way and, therefore, arrays of dislocations are created in the martensite around the precipitates. In fact the Burgers vector suggest that the dislocations form by deformation of martensite [14,15]. The difficulties found by the martensite plates to absorb the precipitates restrict its growth, and thinner plates form, as observed. Sample 3 can be considered an extreme case of restriction in martensite plate growth. Taking into account the relationship between plate sizes and distribution of precipitates discussed in [7], the smaller plate size can account for the lesser formation of dislocations in the matrix between the precipitates, specially in sample 3.

As mentioned above, the dislocations found in the matrix surrounding the precipitates are formed to accommodate the stresses between the precipitates and the martensite. Therefore, for the subsequent cycles these dislocations favour the formation of the same martensite plate as before, since this plate

should be the best accommodated with the precipitates and surrounding dislocations. In fact, a reproducibility of the plate arrays has been observed in sample 1after 10 cycles.

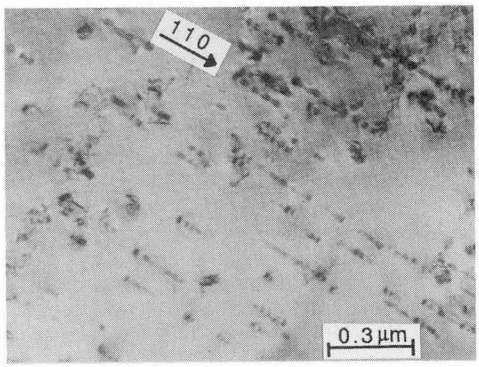

Figure 3. Bright field micrograph from specimen 1 with 200 cycles, showing an area which contains a very small density of dislocations. Zone axis [001], **g**=[110]

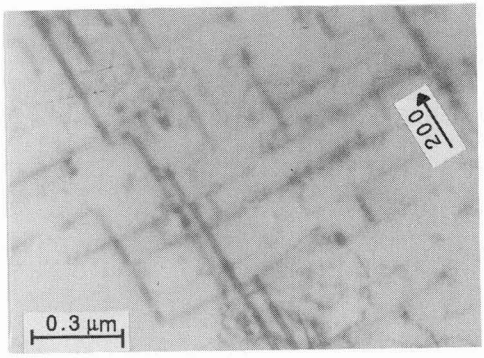

Figure 4. Bright field image from the matrix in between the precipitates in specimen 3 with 200 cycles. Zone axis [011], **g**=[200]

3.4 Effect of cycling on the martensitic transformation

The effect of the dislocations formed during thermal cycling on the martensitic transformation in samples with no precipitates was analysed in [7]. Three contributions were considered: i) the different energy of dislocations when they are embedded in the matrix or in the martensite, ii) the energy of the faults formed in martensite by the existing dislocations whose Burgers vector lies out of the basal plane and iii) the energy of the martensite interfaces, which is higher in the cycled specimens due to a considerable reduction of plate size after cycling. The reduction of plate size is due to the interaction between martensite and the existing dislocations. These effects produce a small inclination and decrease of the whole transformation cycle towards lower temperatures.

In samples containing precipitates the reduction of plate size with cycling does not occur, since in this case the plate size is mainly controlled by the precipitates, which are already present from the first cycle. Thus, the energy of martensite interfaces does not contribute to the effects of cycling on the transformation. But it indeed contribute to the effects of the precipitates on the martensitic transformation, comparing with precipitate-free specimens, since the plate size is much lower. This added interfacial energy present in the martensitic state leads to a shift of the whole transformation to lower temperatures with respect to precipitate-free samples.

On the other hand, an additional contribution has to be taken into account, which is related to the better accommodation of the martensite and the precipitates in the cycled samples, due to the dislocations formed around the precipitates. The precipitate accommodation involve an extra energy present in the martensitic phase and, then, shifts the transformation to lower temperatures and increase the Ms-Mf difference [9,10] in the first cycles. After cycling, this extra energy and their related effects are reduced.

In samples 1 and 2, the latter contribution would be small and comparable with the effect of the dislocations formed in between the precipitates. A compensation between both opposites effects exists, which leads to the high transformation stability (absence of evolution) during cycling. In sample 3, the reduction in the accommodation energy is not compensated by the weaker effect of dislocations.

Acknowledgements

J. Pons acknowledges the DGICyT (MEC, Spain) for the concession of a grant of the PFPI. Partial financial support from CICyT (project num. MAT89-0407-C03-03) is also acknowledged.

References

[1] TADAKI T., TAKAMORI M., SHIMIZU K.; *Trans. of Japan Inst. of Metals* **28** (1987) 1202.
[2] PERKINS J., MUESING W.E.; *Metall. Trans. A* **14A** (1983) 33
[3] PERKINS J., BOBOWIEC P.; *Metall. Trans. A* **17A** (1986) 195
[4] AUGUET C., CESARI E., MAÑOSA LL.; *J. Phys. D. Appl. Phys.* **22** (1989) 1712
[5] RIOS-JARA D., MORIN M., ESNOUF C., GUENIN G.; *Scripta Metall.* **19** (1985) 441
[6] RIOS-JARA D., GUENIN G.; *Acta Metall.* **35** (1987) 109
[7] PONS J., LOVEY F.C., CESARI E.; *Acta Metall. Mater.* **38** (1990) 2733
[8] RAPACIOLI R., CHANDRASEKARAN M.; *Proc. Int. Conf. on Martensitic Transf.* (The Inst. of Metals) 1979, p. 596
[9] AUGUET C., CESARI E., RAPACIOLI R., MAÑOSA LL.; *Scripta Metall.* **23** (1989) 579
[10] PONS J., CESARI E.; *Thermoch. Acta* **145** (1989) 237
[11] PONS J., CESARI E., ROCA M.; *Mater. Letters* **9** (1990) 542
[12] LOVEY F.C., CHANDRASEKARAN M.; *Acta Metall.* **31** (1983) 1919
[13] LOVEY F.C., CESARI E., AUGUET C., MAÑOSA LL., RAPACIOLI R.; *Mater. Sci. Forum* **56-58** (1990) 493
[14] MARUKAWA K., KAJIWARA S.; *Phil. Mag.* **A55** (1987) 85
[15] SADE M., URIBARRI A., LOVEY F.C.; *Phil. Mag.* **A55** (1987) 445